

Preprint Numbers: UNITU-THEP-15/1994
TU-GK-94-003

Analytic Structure of the Quark Propagator in a Model with an infrared vanishing Gluon Propagator

Axel Bender* and Reinhard Alkofer†

**Physics Division, Argonne National Laboratory,
Argonne, Illinois 60439-4843, USA*

*†Institut für Theoretische Physik, Universität Tübingen,
Auf der Morgenstelle 14, D-72076 Tübingen, FRG*

Abstract

The Dyson-Schwinger equation for the quark self energy is solved in rainbow approximation using an infrared (IR) vanishing gluon propagator that introduces an IR mass scale b . There exists a b dependent critical coupling indicating the spontaneous breakdown of chiral symmetry. If one chooses realistic QCD coupling constants the strength and the scale of spontaneous chiral symmetry breaking decouple from the IR scale for small b while for large b no dynamical chiral symmetry breaking occurs. At timelike momenta the quark propagator possesses a pole, at least for a large range of the parameter b . Therefore it is suggestive that quarks are not confined in this model for all values of b . Furthermore, we argue that the quark propagator is analytic within the whole complex momentum plane except on the timelike axis. Hence the naïve Wick rotation is allowed.

to appear in Phys. Rev. D

Pacs Numbers: 12.38.Aw, 11.30.Qc, 12.38.Lg

Typeset using REVTeX

I. INTRODUCTION

New accelerators like CEBAF, MAMI-B and COSY will investigate hadron observables at a scale intermediate to the low-energy region where hadron phenomena mainly reflect the underlying principles of chiral symmetry and its dynamical breakdown and to the high momentum region where the “strong” interaction has the appearance of being a perturbation on free-moving quarks and gluons. A reasonable theoretical description of intermediate energy physics therefore has to satisfy at least the following requirements: Formulated in terms of quarks and gluons it has to account for a mechanism of dynamical chiral symmetry breaking (DCSB) and identify the related Goldstone bosons in the measured spectrum of quark bound states. In addition, all the correlation functions have to transform properly under the renormalization group of Quantum Chromo Dynamics (QCD), *i.e.* at large momenta one should recover the correct anomalous dimensions. Only if these requirements are fulfilled the theoretical framework is fast in those grounds of the theory of strong interaction that are well established. Furthermore, it is desirable to formulate a microscopic picture of the cause of confinement.

In this context growing interest has been focused on the Euclidean Dyson–Schwinger equations (DSE’s) as a tool for developing and applying non-perturbative methods in quantum field theories, a recent review on this subject is given in Ref. [1]. Realistic models of QCD derived through truncation of the DSE tower are *applicable in the whole Euclidean momentum space* and, among others, have the following features: Quark condensation gives rise to DCSB, the chiral Goldstone bosons are identified with the lowest mass pseudoscalar quark-antiquark bound states, perturbative QCD is matched at large momenta, and a study of the analytic structure of the quark propagator provides some insight into the mechanism of confinement.

The DSE’s include the Bethe-Salpeter equations (BSE’s) for bound states, especially the ones describing physical mesons [2]. The BSE’s are coupled to the DSE’s for the quark and gluon propagators, *i.e.* the BSE’s need as input at least the full renormalized quark and gluon propagators which — for calculating the meson mass spectrum, for instance — have to be known at complex Euclidean momenta far away from the real axis. In principle, the quark and gluon propagators can be determined from their DSE’s. As these are coupled to the infinite tower of DSE’s one is not able to solve the equations exactly. Possible approximation schemes are based on the truncation of the DSE tower: Some n -point functions like the gluon propagator and the quark-gluon vertex are parametrized choosing *Ansätze* such that certain requirements are fulfilled. Important constraints are imposed by the discrete and continuous symmetries of QCD most of which are formulated in Ward or Slavnov-Taylor identities. Additional input may be taken from hadron phenomenology.

In this paper we investigate the analytic structure of the quark propagator using the Euclidean DSE for the quark self energy in rainbow approximation where the full quark-gluon vertex is replaced by the perturbative one. The main ingredient for our study is a color diagonal gluon propagator whose transverse part vanishes at zero four momentum:

$$D_T^{\text{IR}}(k^2) = \frac{k^2}{k^4 + b^4} . \quad (1)$$

Herein k denotes the (spacelike) gluon momentum and b is an energy scale to be determined. This form of the gluon propagator is motivated by very distinct considerations. One is based

on the complete elimination of Gribov copies within a lattice formulation of non-abelian gauge theories [3]: Landau gauge is fixed uniquely with the help of a ‘thermodynamic parameter’. The resulting functional integral is dominated by field configurations on the Gribov horizon. This implies that the gluon propagator vanishes for small momenta k as k^2 . In a couple of different studies a gluon propagator of the form (1) is obtained by considering a generalized perturbative expansion of the seven superficially divergent proper vertices of QCD which are allowed to depend non-analytically on the coupling constant [4]. Furthermore, the Field Strength Approach (FSA) to QCD supports the form (1) for being the dominant part of the infrared quark-quark interaction [5]; however, the color structure of the FSA gluon propagator is not diagonal. At last, some recent lattice calculations obtained a gluon propagator which allow a fit of the form (1) (but which do not rule out a fit using a standard massive particle propagator) [6].

As the gluon propagator (1) has no poles for timelike momenta it may be argued that it describes confined gluons. Instead, the gluon propagator has poles on the imaginary axis, $k^2 = \pm ib^2$, and therefore the gluon ‘decays’ after some time $\tau \approx 1/b$. This can be interpreted as the gluons being screened. On the other hand, the gluon propagator (1) is smaller than the perturbative one for all momenta: $k^2/(k^4 + b^4) < 1/k^2$. This has drastic consequences for DCSB as we will show: For the values of b that are suggested by the lattice studies of Ref. [6] chiral symmetry will be realized in the Nambu-Goldstone mode for unrealistic large coupling constants only. We also find that quarks are not confined in this model, at least for a large range of model parameters b .

A similar study was undertaken by Hawes et al. [7]. In this work the gluon propagator (1) and a non-trivial quark-gluon vertex has been used to calculate the quark propagator in the spacelike region. Their results are similar to ours, especially they find unconfined quarks. In contrast to our work where the analytic continuation to timelike momenta is performed explicitly and a pole signaling free massive quasi quarks as asymptotic states is found, Hawes et al. use a test for confinement employing a Fourier transformation of the quark Schwinger functions. The large time behavior of these Fourier transforms indicate asymptotic states of massive deconfined quarks.

In Sec. 2 we present our model DSE for the quark self energy. We also discuss the *Ansatz* Eq. (1) for the gluon propagator in more detail. In Sec. 3 we present the numerical solution for the quark self energy at real Euclidean momenta and discuss the dynamical breaking of chiral symmetry. In Sec. 4 we describe the analytic continuation of the quark self energy with special emphasis on its pole structure and the Wick rotation from Euclidean to Minkowski space. In Sec. 5 we conclude.

II. DYSON-SCHWINGER EQUATION FOR THE QUARK SELF ENERGY

Our starting point is the DSE for the QCD quark two-point function in Euclidean momentum space which can be written in terms of the quark self energy $\Sigma(p)$. After renormalization it reads [8]:

$$\Sigma(p) = (1 - Z_2)\gamma \cdot p + (Z_2 Z_m - 1)m + Z_1 C_F g^2 \int \frac{d^4 q}{(2\pi)^4} D_{\mu\nu}(p - q) \Gamma_\mu(p, q) S(q) \gamma_\nu \quad (2)$$

with $C_F = (N_C^2 - 1)/(2N_C) = 4/3$ for three colors and g denoting the QCD coupling constant. m is the current quark mass. $Z_1(\mu^2, \Lambda^2)$, $Z_2(\mu^2, \Lambda^2)$ and $Z_m(\mu^2, \Lambda^2)$ are renormalization constants depending on a regularization parameter Λ and getting fixed at the renormalization point $p^2 = \mu^2$.

The three Green's functions that appear on the r.h.s. of Eq. (2) are

1. the quark propagator,

$$S(q) = \frac{1}{\gamma \cdot q - m - \Sigma(q)} = \frac{1}{\gamma \cdot q A(q^2) - B(q^2)} = \frac{Z(q^2)}{\gamma \cdot q - M(q^2)}, \quad (3)$$

with B and A denoting the scalar and vector parts of the quark self energy Σ , respectively, and Z and M the field renormalization function and the mass function, respectively;

2. the gluon propagator

$$D_{\mu\nu}(k) = \left(\delta_{\mu\nu} - \frac{k_\mu k_\nu}{k^2} \right) D_T(k^2) + \xi \frac{k_\mu k_\nu}{k^4} \quad (4)$$

where only the transverse piece, D_T , is dressed due to vacuum polarization and

3. the quark-gluon vertex $\Gamma_\mu(p, q)$.

Of course, the gauge parameter ξ appearing in the gluon propagator (4) is a function of the renormalization point μ^2 , *i.e.* any redefinition of the renormalization point leads to a new gauge. The only gauge which is not affected by renormalization is the fix point $\xi = 0$, *i.e.* Landau gauge [9,10]. In our studies we therefore concentrate on this case.

For studying Eq. (2) one has to put in the full gluon propagator and the full quark-gluon vertex; an exact investigation of the quark DSE (2) therefore requires solving their DSE's, too. To do so the gluon 3- and 4-point functions, the ghost self energy, the quark-quark scattering kernel, and so on, have to be known. Each of them again fulfills its own DSE. We do not address the problem of solving all these DSE's simultaneously but instead truncate the infinite tower of DSE's by making *Ansätze* for both the gluon propagator as well as the quark-gluon vertex.

Neglecting ghost contributions to the gluon vacuum polarization the transverse part of the gluon propagator (4), $D_T(k^2)$, is closely related to the running coupling constant of QCD, $\alpha(k^2)$:

$$g^2 D_T(k^2) = \frac{4\pi\alpha(k^2)}{k^2}. \quad (5)$$

In addition,

$$Z_1(\Lambda_{\text{UV}}, \mu^2) = Z_2(\Lambda_{\text{UV}}, \mu^2) \quad (6)$$

in Landau gauge; this is a result of the Ward identity that connects the quark-gluon vertex to the inverse of the quark propagator.

Taking into account one-loop corrections to the QCD perturbation expansion one possible smooth interpolation between IR and UV behavior is the following *Ansatz* for the gluon propagator:

$$g^2 D_T(k^2) = D_T^{\text{IR}}(k^2) \frac{\lambda}{\log(\tau + k^2/\Lambda_{\text{QCD}}^2)} \quad (7)$$

with Λ_{QCD} the QCD scale parameter and λ the coupling strength which is related to the anomalous dimension of the quark mass, $d_M = 12/(33 - 2N_f)$ [14,15]: $\lambda = 4\pi^2 d_M$. However, in our numerical studies we will treat λ as an adjustable parameter. Furthermore, we set $\tau \equiv e$ to ensure that the whole strength of the infrared (IR) quark-quark interaction is carried by the function $D_T^{\text{IR}}(k^2)$. In the following we will call the second factor on the r.h.s. of Eq. (7) ‘ultraviolet (UV) improvement’. Note that in Eq. (7) the four-momentum k is assumed to be spacelike. We like to mention that its continuation to large complex momenta is by no means fixed by the behavior in the asymptotic spacelike region. For example one could replace

$$\frac{\pi d_M}{\ln(\tau + k^2/\Lambda_{\text{QCD}}^2)} \rightarrow \frac{2\pi d_M}{\ln(\tau^2 + k^4/\Lambda_{\text{QCD}}^4)} \quad (8)$$

without altering the spacelike UV behavior. Indeed, both expressions are quite similar even for small spacelike four-momenta. On the other hand, their analytic properties are very different. While the function on the left hand side has its cut on the timelike axis, $k \in i\mathbb{R}$, the one on the right hand side has cuts for $k \in \sqrt{\pm i}\mathbb{R}$.

Of course, one can use a two- or a three-loop order running coupling of QCD instead of the UV-improvement in Eq. (7). Nevertheless, even these cannot provide information about the structure of the gluon propagator at small spacelike momenta (≤ 2 GeV). Hence, for proceeding a parametrization of D_T^{IR} is unavoidable.

On the parametrization of the IR part of the gluon propagator a great deal of work has been done during the last years. Several parametrizations have been investigated and have supported the opinion that quark confinement is closely related to infrared slavery or at least to a strong finite quark-quark interaction in the infrared momentum regime. Nevertheless, as remarked in the Introduction, there exist very distinct studies [3], [4] (using Landau gauge) and [5] that propose

$$D_T^{\text{IR}}(k^2) = \frac{k^2}{k^4 + b^4} \quad (9)$$

with a dynamical mass scale b assumed to be proportional to Λ_{QCD} . In addition, Refs. [3,5] even argue that $b \approx \Lambda_{\text{QCD}}$. This propagator has no Källén–Lehmann representation [16] indicating that the propagation of a free quasi gluon is not possible. As the strength of the quark-quark interaction vanishes at small momenta (corresponding to large distances in coordinate space) the solution of the quark DSE (2) with the gluon propagator (9) as input would exhibit a new mechanism for quark confinement *if any*.

For simplicity we use the rainbow approximation, *i.e.* we formally replace the dressed by the perturbative quark-gluon vertex in Eq. (2):

$$\Gamma_\mu(p, q) = \gamma_\mu. \quad (10)$$

In this approximation the solutions of the Bethe–Salpeter equations (BSE’s) for color-singlet quark-antiquark bound states show the correct low energy behavior as formulated in current algebra and partial conserved axial current (PCAC) relations. For instance, the quark bound states carrying the quantum numbers of the pseudoscalar mesons can be identified

with the Goldstone bosons related to the dynamical breakdown of the $SU_R(N_f) \times SU_L(N_f)$ chiral symmetry of massless QCD [11]; in case of massive QCD the pion mass is determined by a generalized Gell-Mann–Oakes–Renner relation. The rainbow and the separable approximation [12] are the only known approximations that imply the foregoing consistent formulation of quark–DSE and BSE for mesons. Furthermore, the rainbow approximation (10) is equivalent to the stationary phase approximation of the global color-symmetry model (GCM) [13], an abelianized version of QCD with quark fields being transformed to collective fields composed of quarks and anti-quarks and carrying the quantum numbers of mesonic fields.

After inserting Eqs. (9) and (10) (together with or without Eq. (7)) into Eq. (2), using Eq. (6) and fixing the renormalization point, μ^2 , such that vector and scalar part of the quark self energy obey the renormalization conditions

$$A(p^2 = \mu^2) = \alpha , \quad (11)$$

$$B(p^2 = \mu^2) = \beta \quad (12)$$

with constants α and β being fixed later, we get two integral equations which couple the functions A and B that now depend on the momentum $s = p^2$, the renormalization point μ^2 , and the regularization parameter Λ_{UV}^2 :

$$A(s, \mu^2; \Lambda_{\text{UV}}^2) = \alpha \frac{1 - J_A[A, M](s, \mu^2; \Lambda_{\text{UV}}^2)}{1 - J_A[A, M](\mu^2, \mu^2; \Lambda_{\text{UV}}^2)} , \quad (13)$$

$$B(s, \mu^2; \Lambda_{\text{UV}}^2) = \beta + \alpha \frac{J_B[A, M](s, \mu^2; \Lambda_{\text{UV}}^2) - J_B[A, M](\mu^2, \mu^2; \Lambda_{\text{UV}}^2)}{1 - J_A(\mu^2, \mu^2; \Lambda_{\text{UV}}^2)} \quad (14)$$

with

$$J_A[A, M](s, \mu^2; \Lambda_{\text{UV}}^2) = \frac{\lambda}{6\pi^3} \int_0^{\Lambda_{\text{UV}}^2} \frac{dr}{A(r, \mu^2; \Lambda_{\text{UV}}^2)[r + M^2(r, \mu^2; \Lambda_{\text{UV}}^2)]} \int_{-1}^1 dx I_A(x; r, s) \Xi(x; r, s) , \quad (15)$$

$$J_B[A, M](s, \mu^2; \Lambda_{\text{UV}}^2) = \frac{\lambda}{6\pi^3} \int_0^{\Lambda_{\text{UV}}^2} \frac{dr M(r, \mu^2; \Lambda_{\text{UV}}^2)}{A(r, \mu^2; \Lambda_{\text{UV}}^2)[r + M^2(r, \mu^2; \Lambda_{\text{UV}}^2)]} \int_{-1}^1 dx I_B(x; r, s) \Xi(x; r, s) \quad (16)$$

where

$$\Xi(x; r, s) = \begin{cases} 1 & \text{without} \\ \left[\log \left(\tau + r + s - 2x\sqrt{rs}/\Lambda_{\text{QCD}}^2 \right) \right]^{-1} & \text{with UV improvement, Eq. (7).} \end{cases} \quad (17)$$

The functions I_A and I_B are defined in the appendix, Eqs. (A1) and (A2), where also the analytic expressions for the angle integrals (x -integrals) in case of $\Xi = 1$ are given (Eqs. (A3) and (A4)). The mass function in Eqs. (13) and (14) reads:

$$M(s, \mu^2; \Lambda_{\text{UV}}^2) = \frac{B(s, \mu^2; \Lambda_{\text{UV}}^2)}{A(s, \mu^2; \Lambda_{\text{UV}}^2)} = \frac{\beta [1 - J_A(\mu^2, \mu^2, \Lambda_{\text{UV}}^2)] + \alpha [J_B(s, \mu^2; \Lambda_{\text{UV}}^2) - J_B(\mu^2, \mu^2; \Lambda_{\text{UV}}^2)]}{\alpha [1 - J_A(s, \mu^2, \Lambda_{\text{UV}}^2)]} . \quad (18)$$

To make contact with perturbative QCD one has to formulate an appropriate renormalization condition ensuring the asymptotic freedom of quarks. It is convenient to choose the renormalization point as large as possible and set

$$\alpha = 1 , \quad (19)$$

$$\beta = m \quad (20)$$

at this point. The largest available momentum is $s = \Lambda_{\text{UV}}^2$; therefore we set: $\mu^2 \equiv \Lambda_{\text{UV}}^2$ if not stated otherwise.

Numerically, it turns out that $J_A[A, M](\mu^2, \mu^2; \Lambda_{\text{UV}}^2)$ is very small for μ^2 being large enough. Actually, in the limit $\mu^2 \rightarrow \infty$ it vanishes exactly. Hence, solving the DSE (13) and (14) for the renormalized quark self energy is (within numerical accuracy) identical to solving the equations

$$A(s, \mu^2; \Lambda_{\text{UV}}^2) = 1 - J_A[A, M](s, \mu^2; \Lambda_{\text{UV}}^2) , \quad (21)$$

$$B(s, \mu^2; \Lambda_{\text{UV}}^2) = \widehat{m}(\mu^2) + J_B[A, M](s, \mu^2; \Lambda_{\text{UV}}^2) , \quad (22)$$

when imposing the renormalization condition

$$M(s, \mu^2; \Lambda_{\text{UV}}^2) = \frac{mA(\mu^2, \mu^2; \Lambda_{\text{UV}}^2) + B(s, \mu^2; \Lambda_{\text{UV}}^2) - B(\mu^2, \mu^2; \Lambda_{\text{UV}}^2)}{A(s, \mu^2, \Lambda_{\text{UV}}^2)} . \quad (23)$$

\widehat{m} is a running current mass

$$\widehat{m}(\mu^2) = m - J_B[A, M](\mu^2, \mu^2; \Lambda_{\text{UV}}^2) . \quad (24)$$

We like to remark that in case of the DSE system (21,22) this condition is sufficient because the approximation $J_A(\mu^2, \mu^2; \Lambda_{\text{UV}}) = 0$ sets the renormalization constant $Z_2(\mu^2; \Lambda_{\text{UV}}) = 1$. For the system (13,14) Z_2 has to be fixed dynamically and hence two constraints, Eqs. (11) and (12), are needed.

Asymptotic behavior of the quark self energy

At large spacelike momenta s the IR mass scale b in the gluon propagator (9) can be neglected and the integral equations (13) and (14) with $\Xi = 1$ (*i.e.* no UV improvement) can be converted into differential equations [20]. As for large s the integral $J_A[A, M](s, \mu^2, \Lambda_{\text{UV}}^2)$ becomes very small the vector part of the quark self energy is approximatly equal to 1 and hence $Z_2 \approx 1$. The scalar part B is then determined by the non-linear differential equation

$$s \frac{d^2 B}{ds^2} + 2 \frac{dB}{ds} + \frac{\lambda}{4\pi^2} \frac{B}{s + B^2} = 0 \quad (25)$$

with the boundary condition formulated in Eqs. (12,20). If there exists a bounded solution one can drop the term B^2 in the denominator and one gets the asymptotic solution

$$\frac{B(s)}{B(0)} \xrightarrow{s \text{ large}} \frac{a}{\sqrt{s/\mu^2}} \left\{ \cos \left[\frac{\kappa}{2} \ln \left(s/\mu^2 \right) + \varphi \right] \right\} \quad (26)$$

with $\kappa = \sqrt{\lambda/\lambda_C - 1}$. $\lambda_C = \pi^2 \approx 9.87$ is (up to a trivial color factor $C_F^{-1} = 3/4$) the critical coupling of Quantum Electro Dynamics (QED). Implying the UV boundary condition (20) one gets

$$\varphi = \arccos \frac{m}{a} . \quad (27)$$

The parameter a is uniquely fixed by the IR boundary condition *i.e.* by the solution of the integral equation (14) which determines the slope of B at the renormalization point μ^2 .

In case of the UV improved model as defined by the gluon propagator (7) the asymptotic behavior of the mass function $M(s)$ differs qualitatively from Eq. (26). An analysis based on the renormalization group yields [14,1]:

$$M(s) \xrightarrow{s \text{ large}} -\frac{\lambda}{3} \langle \bar{q}q \rangle_{\mu^2} \frac{1}{s} \frac{\left[\log \left(\mu^2 / \Lambda_{\text{QCD}}^2 \right) \right]^{-\lambda/4\pi^2}}{\left[\log \left(s / \Lambda_{\text{QCD}}^2 \right) \right]^{1-\lambda/4\pi^2}} . \quad (28)$$

Dynamical Chiral Symmetry Breaking

Compared to the hadronic mass scale Λ_{QCD} the up and down quark current masses m are negligible. In the limit of zero current masses, $m = 0$, the QCD Lagrangian is invariant under chiral transformations. The Wigner-Weyl realization of the vacuum state corresponds to the trivial solution of Eqs. (13) and (14):

$$B_{\text{trivial}}(s, \mu^2, \Lambda_{\text{UV}}^2) = 0 . \quad (29)$$

In QED in Landau gauge this trivial solution *maximizes* the CJT action [17] whose stationary phase condition is identical to the quark DSE (2) [18,19]. This statement holds also true for abelianized QCD as long as $A \approx 1$. Hence, a vacuum configuration with $B \neq 0$ will be dynamically favored if $A \approx 1$. This may be tested by evaluating the CJT action at the stationary points.

A nontrivial solution of Eqs. (13) and (14) (in the case $m = 0$) indicates the dynamical breaking of chiral symmetry, *i.e.* the corresponding vacuum state is realized in the Nambu-Goldstone mode. From the definition of the quark condensate

$$\langle \bar{q}q \rangle_{\mu^2} = - \lim_{x \rightarrow 0^+} \text{tr}[S(x, 0) - S_0(x, 0)] \stackrel{m=0}{\equiv} -12 \int \frac{d^4 p}{(2\pi)^4} \frac{B(p^2)}{A^2(p^2)p^2 + B^2(p^2)} \quad (30)$$

it is obvious that a non-vanishing scalar part of the self energy, $B > 0$, leads necessarily to a non-vanishing condensate $\langle \bar{q}q \rangle_{\mu^2} < 0$. The scalar part of the quark self energy at zero momentum, $B(0)$, or, correspondingly, the mass value $M(0)$ is therefore an order parameter of DCSB.

Confinement and the analytic continuation of the quark self energy

The analytic continuation of Eqs. (13) and (14) to complex momenta is very important in the studies of DSE's for the following reasons:

1. A quark propagator whose mass function obeys the relation

$$s_M + M^2(s_M) = 0 \quad (31)$$

and whose renormalization function Z is non-vanishing at $s = s_M < 0$ describes a massive particle which should be detectable in some appropriate experiment. Hence, one way to obtain information about quark confinement is the examination of the pole structure of the

quark propagator after continuing real Euclidean to imaginary momenta, *i.e.* s to $-s$: If there does not exist any momentum s_M for which Eq. (31) is fulfilled, there is no Källén-Lehmann representation for the quark propagator and the described quasi-quark is confined.

2. In order to solve the quark bound state equations (*i.e.* the BSE's for mesons or the Fadde'ev equations for baryons) information about the quark self energy in a large domain of the complex momentum plane is needed. While external momenta (*e.g.* the momentum of a meson close to its mass-shell) can be timelike the loop momentum occurring in the BSE is spacelike. Hence, there appear combinations of spacelike and timelike momenta as arguments of the quark self energy functions A and B ; the analytic continuation of these functions to complex momenta is therefore unavoidable if one wants to describe hadrons others than pions.

3. Studying the analytic properties of the quark self energy provides some insight into the connection of the Euclidean formulation of QCD and QCD in Minkowski space. Recently it has been shown [21] that in models containing both gluon and quark confinement the Wick rotation cannot be performed naively indicating thereby the close relation between confinement and singularities or branch cuts appearing in the quark propagator at some complex Euclidean momenta.

III. QUARK SELF ENERGY FOR SPACELIKE MOMENTA

We have solved Eqs. (13) and (14) by iteration with fixed cutoff Λ_{UV} . Different parametrizations and grid densities of the discretized momentum interval $s \in [0, \Lambda_{\text{UV}}^2]$ have been used. All the results we report herein do not depend on changes of the grid parametrization or further increasements of the grid density.

To check the accuracy of the numerical procedure we first study the asymptotic behavior of the DSE-model without UV-improvement, *i.e.* we set $\Xi = 1$ in Eqs. (13) and (14). At large renormalization points we fix the mass function arbitrarily and fit a tail of the form (26) in the momentum region $(b^2 \ll) \mu^2 \leq s \leq \Lambda_{\text{UV}}^2$ allowing all parameters a , φ and λ_C to get varied.

In Fig. 1 the function $B(s)/B(0)$ is shown for $\lambda = 16$, $\mu = 2^{14}b$, $\Lambda_{\text{UV}} = 2^{18}b$ and $m/B(0) = 0.0153$ together with an asymptotic fit (26) with $a = 0.06858$ and

$$\varphi = 1.3461, \lambda_C = 9.869. \quad (32)$$

A comparison with the calculated values $\lambda_C = \pi^2 \approx 9.870$ and $\varphi = \arccos(m/a) = 1.3461$ shows high accuracy for the numerical solution of Eqs. (13) and (14).

For $\mu^2 \gg b^2$ (and $\mu^2 \gg m^2$) the value of the mass function at zero momentum increases linearly with increasing renormalization point,

$$M(0) \propto \mu, \quad (33)$$

a scaling behavior that is well known from studies of four-dimensional QED [20]. The vector part of the quark self energy, A , tends toward unity while the scalar part B admits an almost constant value of order μ up to $s \approx \mu^2/2$. Obviously, the DSE-model defined by Eqs. (9) and (10) is just an IR-regularised version of four-dimensional QED for $b/\mu \ll 1$.

Modifying the asymptotic behavior of the gluon exchange by taking into account the renormalization group (RG) improved loop-corrections, cf. Eq. (7), introduces a third mass scale: Λ_{QCD} . Hence, no scaling comparable to that of Eq. (33) occurs anymore. Instead, the quark self energy functions A and B show the proper RG transformation properties. For several parameter pairs $(b/\Lambda_{\text{QCD}}, \lambda)$ we have studied the large momentum behavior of the quark mass function M and have found a very good agreement with an asymptotic analysis based on the RG. This is illustrated in Fig. 2 where the calculated mass function for $\lambda = 30$, $b/\Lambda_{\text{QCD}} = 1$, and $\mu/\Lambda_{\text{QCD}} = \Lambda_{\text{UV}}/\Lambda_{\text{QCD}} = 2^{18}$ is shown and an asymptotic tail of the form

$$M(s) = \frac{c}{s} \left[\ln \left(\frac{s}{\mu^2} \right) \right]^{d-1} \quad (34)$$

with

$$c = 1.642 \Lambda_{\text{QCD}}^3 \quad \text{and} \quad d = 0.729 \quad (35)$$

is fitted. The coupling constant λ extracted from this UV tail coincides within 5% with the value inserted into the DSE ($d = \frac{\lambda}{4\pi^2} \approx 0.760$) demonstrating good numerical accuracy. (Note that d is the exponent of a logarithmic term.) The quark condensate in the model characterized by the above parameter set can be calculated from Eq. (28) together with Eq. (35); its value is

$$\langle \bar{q}q \rangle_{\mu^2=1\text{GeV}^2} \approx (-(0.70 \pm 0.03)\Lambda_{\text{QCD}})^3 \approx -((190 \pm 60)\text{MeV})^3. \quad (36)$$

We have used $\Lambda_{\text{QCD}}^{(N_f=4)} = 270 \pm 80$ MeV [22]. The same result is obtained calculating the trace of the quark propagator, Eq. (30): $\langle \bar{q}q \rangle_{\mu^2=1\text{GeV}^2} \approx (-(0.67 \pm 0.02)\Lambda_{\text{QCD}})^3$.

In Fig. 3 the order parameter $M(0)$ is shown as a function of the coupling constant λ . For vanishing current mass, $m = 0$, we have studied the dependence on the renormalisation point μ (here set equal to the cutoff Λ_{UV}) choosing the IR mass scale b equal to Λ_{QCD} as suggested by Refs. [3,5]. The critical behavior of the order parameter, $M(0) \propto (\lambda - \lambda_C)^\beta$ of the solution in the chiral limit gets softened if the current quark mass is non-vanishing, *i.e.* we find the well-known behavior of an order parameter of DCSB. While increasing the regularization parameter Λ_{UV} as well as the renormalization point μ the critical coupling λ_C decreases slightly. The extrapolation $\Lambda_{\text{UV}} \rightarrow \infty$ yields a value of the critical coupling of $\lambda_C = 28.98 \pm 0.02$. As in case of $\lambda > \lambda_C$ the vector part of the quark self energy, A , is quite close to unity, the Nambu-Goldstone phase of DCSB is dynamically favored. The critical exponent extracted from the data is $\beta = 0.59 \pm 0.01$. This value is almost identical to $\beta = 0.57 \sim 0.58$ Hawes *et al.* have derived in their study of the DSE system (21,22) inserting several *dressed* quark-gluon vertices [7].

The critical coupling strongly depends on the IR scale b : Small values of b/Λ_{QCD} lead to small, large ones to large critical coupling constants as one might expect. For $N_F = 0$ (2) the IR scale that yields a critical coupling identical to the coupling suggested by the QCD asymptotics, $\lambda_C \equiv \frac{48}{33}\pi^2$ ($\frac{48}{29}\pi^2$), is $b_{N_F=0(2)}/\Lambda_{\text{QCD}} \approx 0.26 \pm 0.01$ (0.28 ± 0.02). Therefore only for very small IR mass parameters $b \leq 100$ MeV DCSB takes place.

In Fig. 4 the mass functions for different IR parameters b are shown for $\lambda = \frac{48}{29}\pi^2$. The parameter b is varied by two orders of magnitude (for $b/\Lambda_{\text{QCD}} > 0.3$ no DCSB occurs). It is

remarkable that neither the strength of DCSB as “measured” by the order parameter $M(0)$ nor the momentum range that contributes dominantly to the mechanism of DCSB depend on the IR scale b introduced by the effective gluon exchange, *i.e.* the scales of DCSB and the gluon mass scale b are not or only loosely connected to each other if a realistic coupling constant λ is used.

IV. ANALYTIC CONTINUATION OF THE QUARK SELF ENERGY

A. Mass Shell Condition and Constituent Quark Mass

To study quark confinement we will analyze the quark propagator for timelike momenta. Therefore the Euclidean quark self energy has to be continued from spacelike to timelike momenta $p \rightarrow ip$. Correspondingly, the variable $s = p^2$ has to be continued to negative values, $s < 0$.

Eqs. (13) and (14) can be understood as the defining equations for the vector and scalar parts of the quark self energy, A and B , respectively. Therefore the analytic continuation can be performed by smoothly changing the external momenta s while keeping the loop momenta r spacelike. Thus one generates the quark self energy as a function of complex momenta by simply using complex s in Eqs. (13) and (14). Obviously, $A^*(s^*) = A(s)$ and $B^*(s^*) = B(s)$ and hence solving the DSE in the upper half of the complex plane is sufficient. Note that the functions $A(r)$ and $B(r)$ inserted into the right hand side of Eqs. (13) and (14) are still those determined self-consistently on the spacelike momentum axis.

First we generate the functions A and B on a small strip including the positive real axis. There we find that A and B change continuously. No singularities appear and therefore the analytical continuation can be performed patching open sets towards timelike momenta, $s < 0$. Problems arise caused by the poles of the angular integrals $\int dx I_{A/B}(x; r, s) \Xi(x; r, s)$. Those are kinematical singularities that appear for $s_0 \geq \frac{b^2}{2\sin^2\vartheta/2}$ where $s \equiv s_0 \exp(i\vartheta)$ with $s_0 = |s|$. They are integrable as can be seen from the analytic expressions (A3) and (A4) of the appendix, for instance, or from a Laurent series expansion of the kernels (11) and (12). Nevertheless, the numerical results for the domain $s_0 \geq \frac{b^2}{2\sin^2\vartheta/2}$ have been quite unstable against a change of numerical parameters. Hence we restrict our discussion on results for $s_0 < \frac{b^2}{2\sin^2\vartheta/2}$ only. Both functions, A and B , are entire on this domain.

The identification of a mass pole in the quark propagator fulfilling condition (31) is only possible if $b > \sqrt{2}M(-b^2/2)$. This implies that in the case of DCSB our numerical method of identifying such a pole is only reliable for IR mass scale parameters b larger than the created dynamical mass $M(0)$. In this restricted parameter space we find that the mass shell condition (31) for the quark is fulfilled for both models, with and without UV-improvement. *I.e.* close to the momentum $-s_M$ quarks propagate like stable particles with constituent mass $M(-s_M)$. For parameter values $b < \sqrt{2}M(0)$ we are not able to make any statements about the existence of a quark mass pole.

In Figs. 5a and 5b the mass function $M(s)$ in the UV-improved model (7) for $(b/\Lambda_{\text{QCD}}, \lambda) = (0.27, \lambda_{\text{QCD}} = \frac{48}{29}\pi^2)$ and $(1, 30)$, resp., are shown. The parameters used are such that the kinematical singularities are far away from the timelike momentum region

considered here. One recognizes that the mass condition (31) is fulfilled and that the pole mass $\sqrt{s_M}$ is very well approximated by the dynamical mass $M(0)$.

Our result of quark *deconfinement* (obtained for such values of the IR parameter b where our numerical results are stable) is in full agreement with the results of Hawes *et al.* They have investigated the scalar part of the quark Schwinger function, $\Delta_S(T)$, analyzed its asymptotic behavior for large Euclidean times T , and extracted the mass M_{as} of a stable asymptotic fermion state through the relation [7]

$$\lim_{T \rightarrow \infty} \frac{d}{dT} \ln[\Delta_S(T)] = -M_{\text{as}}.$$

M_{as} is found to be (positive) finite and of the order of Λ_{QCD} . While we are using the rainbow approximation (10) for the quark-gluon vertex Hawes *et al.* employ non-trivial vertices. These are constructed in a way that they obey the Ward-Takahashi identity, carry no kinematical singularities, go versus the free vertex for free fields, and ensure the propagators transforming properly under the Landau-Khalatnikov transformations [23,1]. In addition, one of the vertices used in Ref. [7] leads to multiplicative renormalizability [24]. Our study confirms the result of unconfined quarks obtained for an IR vanishing quark-quark interaction [7]. We may also deduce that in this model the form of the quark-gluon vertex is of minor importance (at least, as long as it is free of singularities).

B. Analyticity and Wick rotation

In order to study the analytic properties of the quark propagator we employ Cauchy's integral theorem in the following way. Suppose that the kernels

$$f_A(r; s) \equiv \frac{A(r)}{rA^2(r) + B^2(r)} \int_{-1}^1 dx I_A(x; r, s) \Xi(x; r, s), \quad (37)$$

$$f_B(r; s) \equiv \frac{B(r)}{rA^2(r) + B^2(r)} \int_{-1}^1 dx I_B(x; r, s) \Xi(x; r, s), \quad (38)$$

of the integrals J_A and J_B (cf. Eqs. (15) and (16)) are analytic. Then the integral of $f_{A(B)}$ over a closed contour in the complex momentum plane has to vanish. Due to the renormalization condition (18) the functions $f_{A(B)}$ fall off faster than $1/r^x$ for large r where $x > 1$. Therefore one obtains

$$\int_0^{\Lambda_{\text{UV}}^2} dr f_{A(B)}(r) \approx \int_0^{\Lambda_{\text{UV}}^2} dr e^{i\vartheta} f_{A(B)}(r e^{i\vartheta}) \quad (39)$$

where the difference between the left hand side and the right hand side vanishes for $\Lambda_{\text{UV}} \rightarrow \infty$. This relation implies that the iteration of Eqs. (13) and (14) along a rotated axis should lead to the same values $A(0)$ and $B(0)$ as the iteration along the spacelike axis as long as the kernels $f_{A(B)}$ are analytic. This provides us with an analyticity test for the functions $f_{A(B)}$.

The gluon propagator (9) is symmetric under the exchange of spacelike and timelike momenta:

$$D_T(-k^2) = -D_T(k^2). \quad (40)$$

Even though the UV-improved version of this gluon exchange does not carry the symmetry (40) an UV-improvement with the replacement (8) does. As the spacelike properties (such as dynamical chiral symmetry breaking) are only slightly affected by the replacement (8) we believe our symmetry considerations being quite general and we concentrate on the UV-unimproved form (9) for the gluon propagator alone.

In the following we study the approximate DSE system (21,22) and we drop the dependencies on regularization parameter Λ_{UV} and renormalization point μ . Assuming f_A and f_B being analytic within the whole complex momentum plane the iterations of Eqs. (21) and (22) along the timelike axis

$$\tilde{A}(-s) = 1 + \frac{\lambda}{6\pi^3} \int_0^{\Lambda_{\text{UV}}^2} dr \frac{\tilde{A}(-r)}{r\tilde{A}^2(-r) - \tilde{B}^2(-r)} \int_{-1}^1 dx I_A(x; r, s), \quad (41)$$

$$\tilde{B}(-s) = (m \rightarrow 0) + \frac{\lambda}{6\pi^3} \int_0^{\Lambda_{\text{UV}}^2} dr \frac{\tilde{B}(-r)}{r\tilde{A}^2(-r) - \tilde{B}^2(-r)} \int_{-1}^1 dx I_B(x; r, s) \quad (42)$$

should lead to the same values $A(0)$ and $B(0)$ as the iteration along the spacelike axis.

Obviously,

$$\tilde{A}(-s) = A(s), \quad \tilde{B}(-s) = \pm i B(s) \quad (43)$$

are solutions of Eqs. (41) and (42) if A and B are solutions of Eqs. (21) and (22). In the Nambu-Goldstone realization of the vacuum, $B(0) \neq 0$, the solutions (43) do not obey the analyticity condition $\tilde{A}(0) = A(0)$ and $\tilde{B}(0) = B(0)$. Therefore the kernels f_A and f_B are *not* analytic in the whole complex momentum plane in case of chiral symmetry being broken dynamically. Note that a “usual” mass pole of the quark propagator is sufficient to explain the behavior (43).

The functions f_A and f_B are products of the vector or scalar part of the quark propagator and the angular integral over Euclidean projections of the gluon propagator. We will argue in the following that the non-analyticity of both functions are caused by the quark propagator. For doing this we study the Wigner–Weyl phase of the system, $B(s) \equiv 0$. In that case the self-consistency equation for $A(s) = \alpha_1(s_0, \vartheta) + i \alpha_2(s_0, \vartheta)$ reads:

$$\alpha_1(s_0, \vartheta) + i \alpha_2(s_0, \vartheta) = 1 + \frac{\lambda}{6\pi^2} \int_0^{\Lambda_{\text{UV}}^2} dr \frac{1}{r(\alpha_1(s_0, \vartheta) + i \alpha_2(s_0, \vartheta))} \int_{-1}^1 dx I_A(x; r, s_0 e^{i\vartheta}) \quad (44)$$

with α_1 and α_2 being the real and the imaginary part of $A(s = s_0 e^{i\vartheta})$, respectively. It is straightforward to proof the following symmetries

$$\alpha_{1/2}(s, \pi + \vartheta) = \alpha_{1/2}(s, \vartheta), \quad (45)$$

$$\alpha_1(s, \frac{\pi}{2} - \vartheta) = \alpha_1(s, \vartheta), \quad (46)$$

$$\alpha_2(s, \frac{\pi}{2} - \vartheta) = -\alpha_2(s, \vartheta). \quad (47)$$

Hence it is sufficient to analyze the integral equation (44) for $\vartheta \in [0, \frac{\pi}{2}]$ only.

In Fig. 6 the function $\alpha_1(s_0, \vartheta)$ is shown for $\lambda = 16$ and various angles ϑ . We have used a small cut-off, $\Lambda_{\text{UV}}^2 = 2^8 b^2$. However, the solutions do not depend on a further increase of the cut-off.

of Λ_{UV}^2 as the chiral symmetric solutions do not display the scaling behavior (33) as in the case of the Nambu-Goldstone phase. The numerical error in Fig. 6 is about 1% to 5%; it is largest close to the imaginary axis.

It is obvious that for all the angles ϑ the real parts α_1 at zero momentum ($s = 0$) are identical; the imaginary parts α_2 which are not shown vanish for small momenta within the numerical accuracy. For $\vartheta = \frac{\pi}{2} = 90^\circ$ the iteration of Eq. (44) does not converge due to the (integrable) singularities of the gluon propagator. Nevertheless there is no signature of any further non-analyticity close to the imaginary axis. We therefore conclude that there is a strong indication for the vector part of the quark self energy being analytic. Then the quark propagator has only one pole, namely the one at $s = 0$.

In the Nambu-Goldstone phase, $B(s) \neq 0$, the integral kernels f_A and f_B from Eqs. (37) and (38) are not holomorphic on the whole complex momentum plane either. There has to be a pole contribution from the contour integration in Eq. (39). As the angular integrals over I_A and I_B do not carry a pole singularity the scalar and the vector parts of the quark propagator have at least one pole. If this singularity is not lying on the real axis but within the complex plane the Wick rotation cannot be performed naively. If it is placed on the timelike axis the naïve Wick rotation is allowed as long as the causal behavior of the quark propagator is suitably determined.

We have not found any singularities except the kinematical ones and the mass pole on the real axis. Even though we are not able to draw compulsory conclusions this numerical result strongly indicates that the quark propagator is analytic within the whole complex momentum plane except on the real timelike axis. This statement is also supported by the analysis within different DSE models [21] where it is found that poles of the quark propagators are lying quite close to the real axis.

In addition, the analyticity condition (43) is quite easily understood from a physical point of view. Under the action of the Wick rotation the Euclidean mass term becomes $(-i)$ times the corresponding Minkowski term, a kinetic fermionic term keeps “unmodified”. In terms of the quark propagator functions this reads:

$$B(s_E) \xrightarrow{\text{Wick}} -i B(s_M), \quad (48)$$

$$A(s_E) \xrightarrow{\text{Wick}} A(s_M) \quad (49)$$

where s_E denotes the Euclidean and s_M the corresponding Minkowski four momentum squared close to a mass pole of the quark propagator. In Minkowski space we therefore just recover one of the “solutions” (43) which is not surprising.

Summarizing this section, there are strong indications that the Euclidean quark propagator of the DSE model specified by the gluon exchange (9) can be continued back to Minkowski space. Within a small region around the mass pole (31) the Minkowskian quark propagator has a Källén-Lehmann representation and it therefore resembles the propagator of a massive stable fermion. For a restricted set of parameters we have been able to verify this numerically. Due to the numerical problems associated with the kinematical singularities we are not really able to prove this statement rigorously for all values of the parameter b . Nevertheless, it is the most plausible conclusion drawn from the properties of the functions f_A and f_B as discussed in this section.

V. SUMMARY AND CONCLUSIONS

We have investigated the Euclidean Dyson-Schwinger equation (DSE) for the quark self energy for an infrared vanishing gluon propagator in rainbow approximation. We have found that this model is not appropriate for describing hadron phenomenology due to several reasons. First, dynamical chiral symmetry breaking (DCSB) occurs either for unphysically large coupling constants only or for a small IR scale, $b \ll \Lambda_{\text{QCD}}$. The strength and the scale of DCSB are then independent of b : the spontaneous breakdown of chiral symmetry is mainly driven by the term added to obtain the correct UV behavior and *not* by the infrared part.

In addition, continuation to timelike momenta reveals that the quark propagator possesses a pole. As our numerical method is only reliable for IR mass scale parameters b larger than the created dynamical quark mass (see the discussion in subsection IV A) this pole can be unambiguously identified for such values of b only. To be explicit, we do not claim that there is no pole, we only state that within our method it cannot be found even if it exists.

However, the occurrence of a mass pole in the propagator can be related to the propagation of a stable particle. Therefore it is clear that quarks are not confined in this model, at least for a large range of the IR parameter b . This is in contradiction to results obtained in Ref. [25]. There heavy quarkonia have been studied using a non-relativistic reduction of the gluon propagator (9) together with a quark propagator and a quark-gluon vertex which result from the DSE studies of Ref. [4]. However, in this work the quark-quark interaction (9) has been replaced by a Coulomb potential. The resulting equation for the quarkonium bound states is just a Lippmann-Schwinger equation for hydrogen with the exception that the non-trivial quark propagators of Ref. [4] have been used. These propagators are then probably the reason for the “confining mechanism” described in Ref. [25]. Stated otherwise, the unusual behavior of the quarks have been put in “by hand”. Such a mechanism is not supported by our calculations.

Instead, our results are in accordance with those of Hawes et al. [7] who have studied the quark propagator for spacelike momenta only and have extracted the quark mass from the large time behavior of the Schwinger functions. Additionally, they have used non-trivial quark-gluon vertices. The good quantitative agreement of our results with those of Ref. [7] shows that the rainbow approximation is a good approximation for this model interaction. This can be understood from the fact that the influence of a non-trivial quark-gluon vertex is concentrated in the infrared which for the studied case is suppressed by the infrared vanishing gluon exchange.

Even though a study of the analyticity of the quark propagator is hampered by numerical difficulties we have found convincing evidence for the quark propagator being analytic within the whole complex Euclidean momentum plane except the timelike (negative real) axis. This has two consequences: First, it is possible to perform the naïve Wick rotation. Second, and more important, the model does *not* lead to quark confinement.

ACKNOWLEDGMENTS

We take this opportunity to express our gratitude to Prof. Dr. H. Reinhardt for his support and his interest in this work. We thank Dr. C. D. Roberts for numerous helpful discussions. AB got benefit from the courses and meetings of the Graduiertenkolleg “Hadrons and Nuclei” (DFG contract Mu 705/3); therefore he especially thanks Prof. H. Müther for organising these meetings. He also gratefully acknowledges financial support by the Studienstiftung des deutschen Volkes. This work has also been partly supported by COSY under contract 41170833.

APPENDIX:

The angular integrands in Eqs. (13) and (14) are:

$$I_A(x; r, s) \equiv \sqrt{\frac{r^3}{s}} \sqrt{1-x^2} \frac{2(1+2x^2)\sqrt{rs} - 3x(r+s)}{(r+s-2x\sqrt{rs})^2 + b^4}, \quad (\text{A1})$$

$$I_B(x; r, s) \equiv r\sqrt{1-x^2} \frac{3(r+s-2x\sqrt{rs})}{(r+s-2x\sqrt{rs})^2 + b^4}. \quad (\text{A2})$$

For $\Xi(x; r, s) = 1$ in Eqs. (13) and (14) (*i.e.* no UV improvement for the quark-quark interaction) the x-integral can be evaluated exactly:

$$\begin{aligned} \int_{-1}^1 dx I_A(x; r, s) = & \frac{\pi b^4}{4s^2} - \frac{\pi r b^2}{sy} \left\{ b^2 \left(\frac{(r-s)^2 + b^4}{(r+s)^2 + b^4} - \frac{(r+s)^2 - b^4}{2rs} + \frac{(r+s)^2((r-s)^2 + b^4)}{rs((r+s)^2 + b^4)} \right) w_+ \right. \\ & \left. + \frac{(r+s)((r-s)^2 + 5b^4)}{(r+s)^2 + b^4} w_- \right\}, \end{aligned} \quad (\text{A3})$$

$$\begin{aligned} \int_{-1}^1 dx I_B(x; r, s) = & \frac{3\pi(r+s)}{4s} \\ & - \frac{3\sqrt{2}\pi r}{((r+s)^2 + b^4)y} \left\{ \frac{r+s}{4rs} \left((r-s)^4 + 2b^2(r+s)^2 + b^8 \right) w_+ + b^2((r-s)^2 - b^4)w_- \right\} \end{aligned} \quad (\text{A4})$$

with

$$y = ((r-s)^2 + b^4)^2 + 16rsb^4 + ((r-s)^2 + b^4)\sqrt{((r-s)^2 + b^4)^2 + 16rsb^4}, \quad (\text{A5})$$

$$w_{\pm} = \sqrt{((r+s)^2 + b^4)\sqrt{((r-s)^2 + b^4)^2 + 16rsb^4} \pm (((r+s)^2 + b^4)^2 - 4rs((r+s)^2 - b^4))}. \quad (\text{A6})$$

REFERENCES

EMail alkofer@ptsun1.tphys.physik.uni-tuebingen.de,
 bender@theory.phy.anl.gov

- [1] C.D. Roberts and A.G. Williams, *Dyson-Schwinger equations and their Application to Hadronic Physics*, Progress in Particle and Nuclear Physics, Vol. 33, pp. 477-575, ed. A. Fässler, Pergamon Press, Oxford, 1994.
- [2] Baryons are described by relativistic Fadde'ev equations.
- [3] D. Zwanziger, Nucl. Phys. B **364**, 127 (1991).
- [4] U. Häbel *et al.*, Z. Phys. A – Atomic Nuclei **336**, 423 and 435 (1990).
 M. Stingl, Phys. Rev. D **34**, 3863 (1986); Erratum *ibid. D* **36**, 651 (1987).
 M. Stingl, *A Systematic Extended Iterative Solution for Quantum Chromodynamics*, Universität Münster preprint MS-TPI-94-13.
- [5] L. v. Smekal, Ph.D. thesis, Tübingen University, 1995.
- [6] C. Bernard, C. Parrinello, and A. Soni, Phys. Rev. D **49**, 1585 (1994).
- [7] F.T. Hawes, C.D. Roberts, and A. G. Williams, Phys. Rev. D **49**, 4683 (1994).
- [8] We use negative semidefinite Euclidean metric, $g_{\mu\nu} = -\delta_{\mu\nu}$, $a \cdot b = -\sum_{j=1}^4 a_j b_j \leq 0$ $\forall a = b \in \mathbb{R}^4$. For abbreviation, we nevertheless define the square of a momentum as $q^2 := -q \cdot q \geq 0$. All Euclidean Dirac matrices, γ_μ , are antihermitean and obey the anticommutation relations $\{\gamma_\mu, \gamma_\nu\} = -2\delta_{\mu\nu}$.
- [9] W. Marciano and H. Pagels, Phys. Rep. **36**, 137 (1978).
- [10] L. P. Pascual and R. Tarrach, *QCD: Renormalization for the Practitioner*, Lecture Notes in Physics **194**, Springer–Verlag, Berlin - Heidelberg - New York, 1984.
- [11] R. Delbourgo and M. D. Scadron, J. Phys. G **5**, 1631 (1979).
- [12] C. D. Roberts, private communication.
- [13] R. T. Cahill and C. D. Roberts, Phys. Rev. D **32**, 2419 (1985).
- [14] H. D. Politzer, Nucl. Phys. B **117**, 397 (1976).
- [15] F. J. Ynduráin, *The Theory of Quark and Gluon Interactions*, Springer–Verlag, Berlin - Heidelberg - New York, 1993.
- [16] J. D. Bjorken and S. D. Drell, *Relativistic Quantum Fields*, McGraw–Hill, New York, 1965.
- [17] J. M. Cornwall, R. Jackiw, and E. Tomboulis, Phys. Rev. D **10**, 2428 (1974).
- [18] C. D. Roberts and R. T. Cahill, Phys. Rev. D **33** 1755 (1986).
- [19] D. Atkinson and P. W. Johnson, Phys. Rev. D **35** 1943 (1987).
- [20] R. Fukuda and T. Kugo, Nucl. Phys. B **117**, 250 (1976).
- [21] S. J. Stainsby and R. T. Cahill, Phys. Lett. A **146**, 467 (1990); Int. J. Mod. Phys. A **7** 7541 (1992).
 P. Maris and H. Holties, Int. J. Mod. Phys. A **7**, 5369 (1992).
- [22] Particle Data Group, Phys. Rev. D **50**, 1173 (1994).
- [23] L. D. Landau and I. M. Khalatnikov, Sov. Phys. JETP **2**, 69 (1956).
- [24] D. C. Curtis and M. R. Pennington, Phys. Rev. D **42**, 4165 (1990).
- [25] M. Becker *et al.*, Phys. Lett. B **267**, 261 (1991).

FIGURES

FIG. 1. The scalar part of the quark self energy, $B(s)/B(0)$, is shown as a function of $s = p^2$. The UV-unimproved gluon propagator (9), the coupling strength $\lambda = 16$, and the numerical cut-off $\Lambda_{\text{UV}}^2 = 2^{36}b^2$ have been used. The solid line represents the function obtained by iterating Eqs. (13) and (14). The dashed one is the asymptotic tail (26) fitted at $s = 2^{28}b^2$ with the parameters (32) inserted.

FIG. 2. This figure shows the quark mass function $M(s)$ of the DSE-model with UV-improved gluon propagator (7). The parameters used are: $\lambda = 30$ and $b/\Lambda_{\text{QCD}} = 1$. The solid line represents the function obtained by iterating Eqs. (13) and (14). The dashed one is the asymptotic tail (34) fitted at large momenta s with the parameters (35) inserted.

FIG. 3. In this figure the order parameter $M(0)$ is shown as a function of the coupling strength λ for the model with the UV-improved gluon propagator (7) and $b/\Lambda_{\text{QCD}} = 1$. The thick lines represent solutions of the DSE (13) and (14) for vanishing quark current mass, $m = 0$, and different renormalization points $\mu^2 = \Lambda_{\text{UV}}$. The thin lines are solutions for different current masses and fixed $\mu^2/\Lambda_{\text{QCD}}^2 = \Lambda_{\text{UV}}^2/\Lambda_{\text{QCD}}^2 = 2^{36}$.

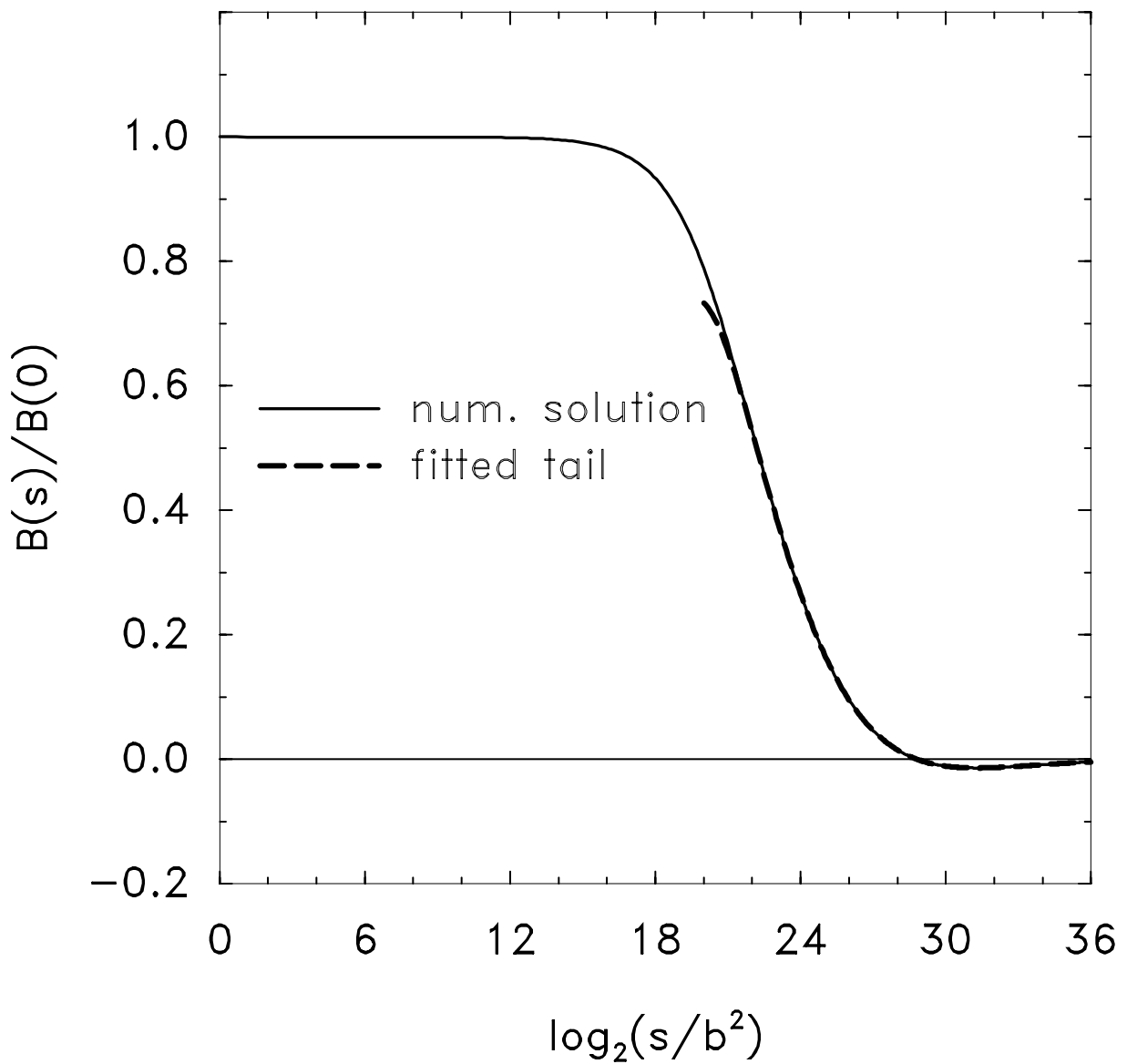
FIG. 4. In this figure the quark mass functions for different IR parameters b are shown. The UV-improved gluon propagator is used and the coupling strength is $\lambda = \frac{48}{29}\pi^2$. The momentum range that contributes dominantly to the breaking of chiral symmetry is defined as the value of s where $M(s) = \frac{1}{2}M(0)$.

FIG. 5. The quark mass function at spacelike and timelike momenta for $(b/\Lambda_{\text{QCD}}, \lambda) = (0.27, \lambda_{\text{QCD}} = 48/(29\pi^2))$ and $(1, 30)$ are shown in Figs. a and b, resp. The thin line on the timelike side of the graphs is the function $\sqrt{-s}$. The point of intersection of this function with the mass functions gives the value of s where the pole condition (31) is fulfilled.

FIG. 6. In this figure the real part α_1 of the scalar quark self energy A is shown for the Wigner-Weyl phase of the DSE model defined by the gluon exchange (9). The different functions correspond to solutions of Eq. (44) iterated along different axes in the Euclidean momentum plane characterized by the angle ϑ .

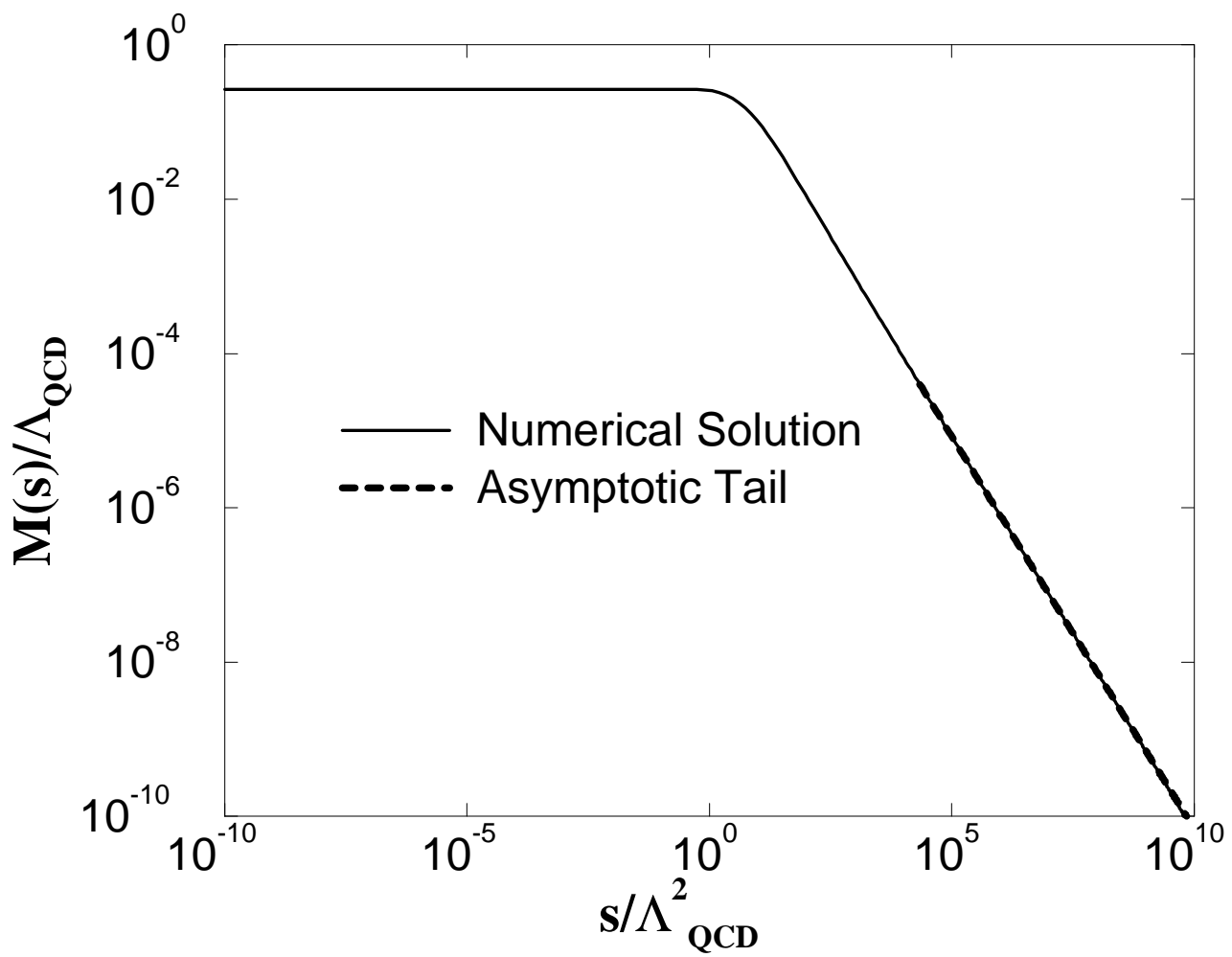
This figure "fig1-1.png" is available in "png" format from:

<http://arxiv.org/ps/hep-ph/9411266v3>



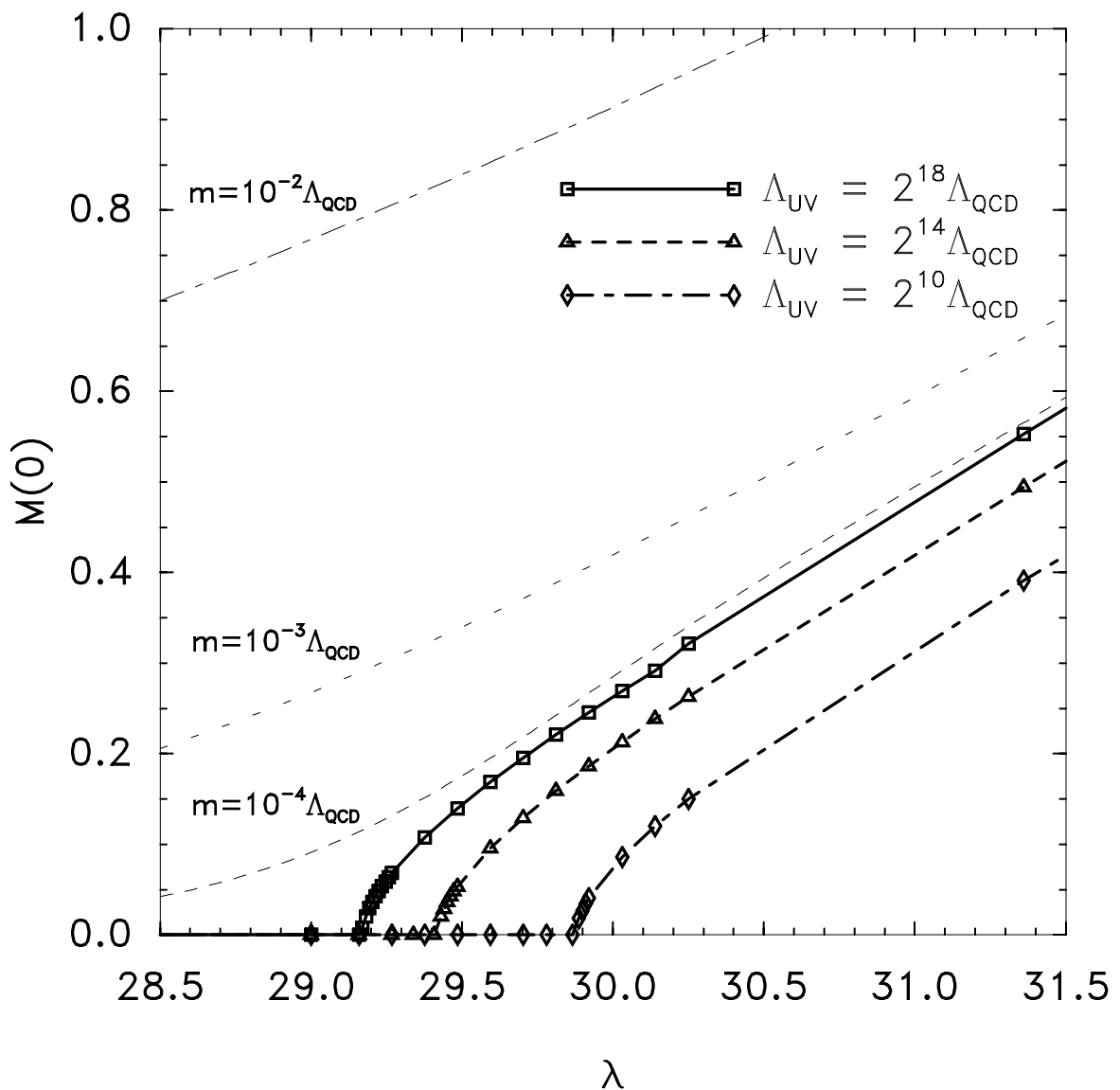
This figure "fig1-2.png" is available in "png" format from:

<http://arxiv.org/ps/hep-ph/9411266v3>



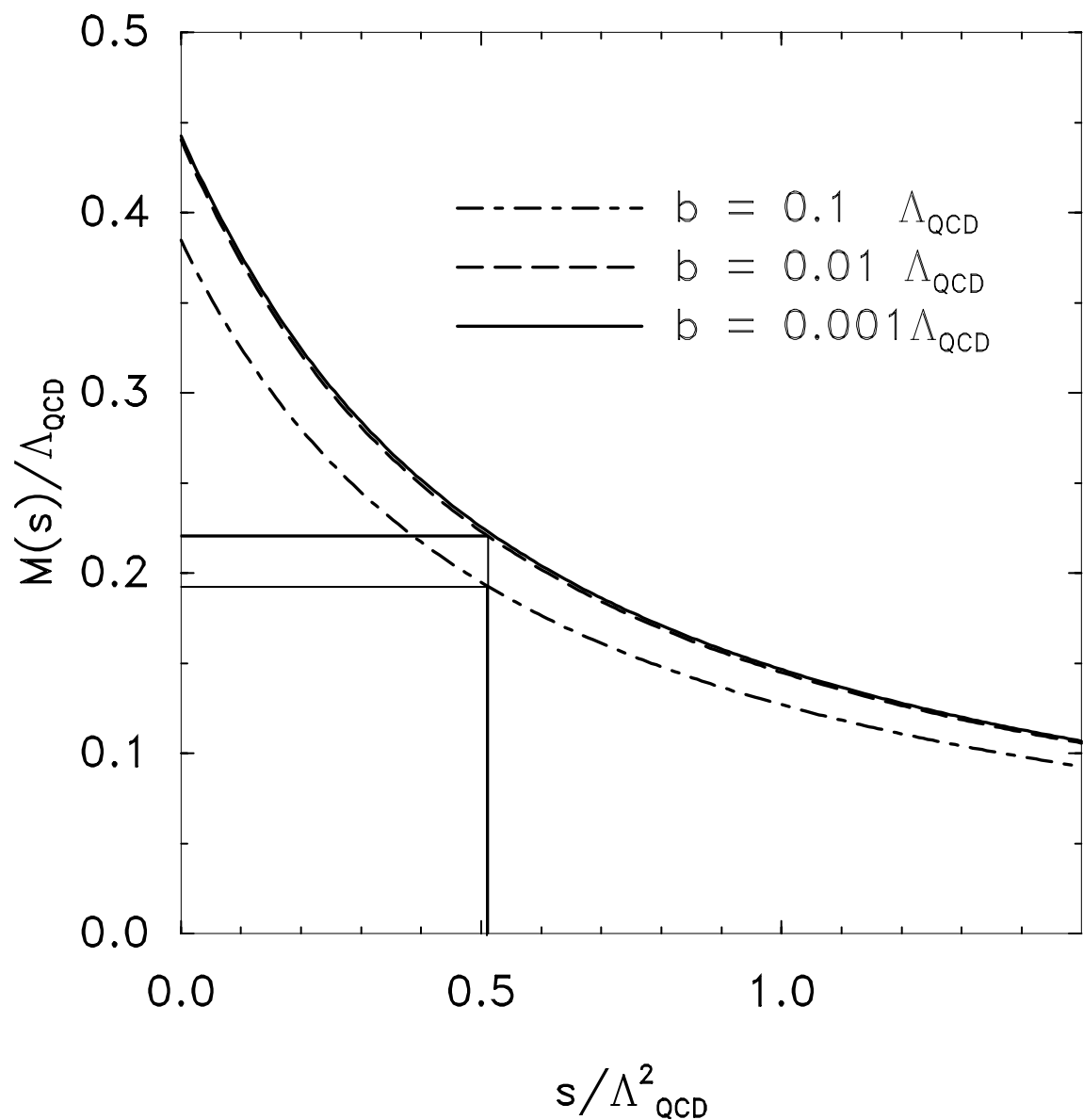
This figure "fig1-3.png" is available in "png" format from:

<http://arxiv.org/ps/hep-ph/9411266v3>



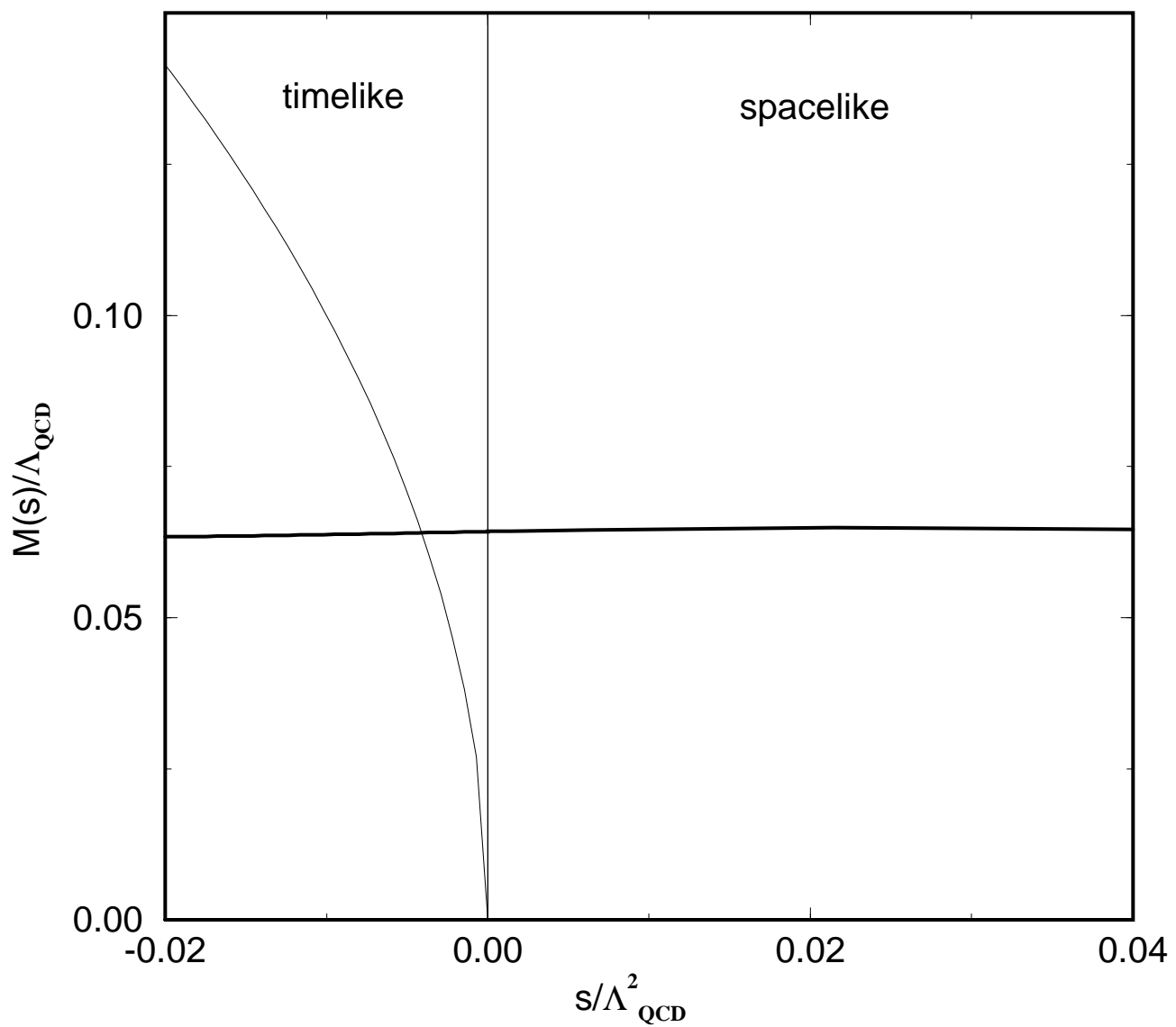
This figure "fig1-4.png" is available in "png" format from:

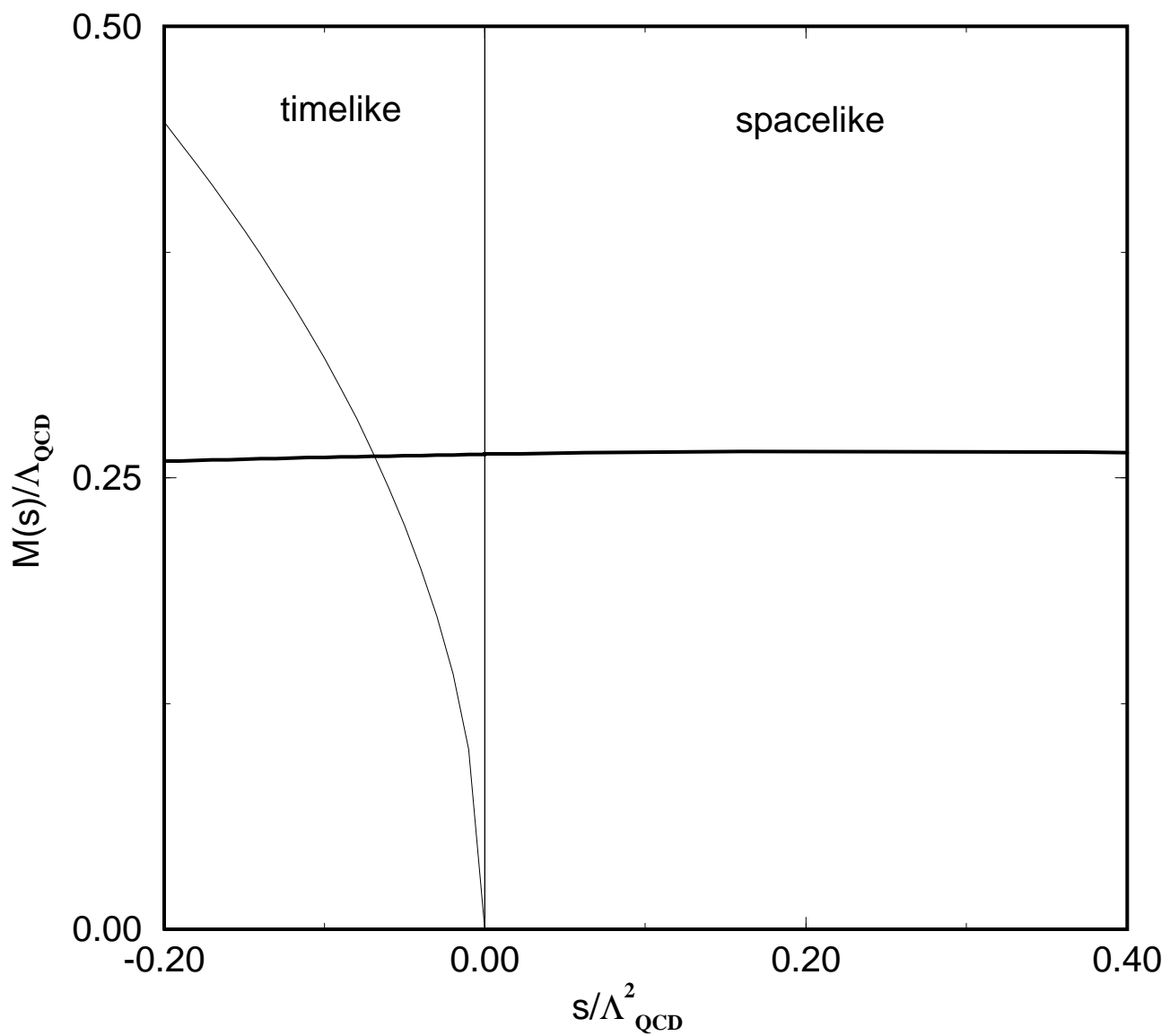
<http://arxiv.org/ps/hep-ph/9411266v3>



This figure "fig1-5.png" is available in "png" format from:

<http://arxiv.org/ps/hep-ph/9411266v3>





This figure "fig1-6.png" is available in "png" format from:

<http://arxiv.org/ps/hep-ph/9411266v3>

